JOURNAL OF SPACECRAFT AND ROCKETS
Vol. 42, No. 2, March–April 2005

Orbit Transfer via Tube Jumping in Planar Restricted Problems of Four Bodies

Hideaki Yamato* and David B. Spencer†
Pennsylvania State University, University Park, Pennsylvania 16802

In the circular-restricted three-body system, there exist bundles of solution orbits, involving a close encounter with the second primary, inside invariant manifolds of libration point orbits. Under the influence of perturbing forces, these trajectory bundles change their locations and distributions, but still exist as bundles, serving as low-energy passageways and forming a network of transportation tubes. Taking full advantage of these transportation mechanics, orbit transfers within planetary systems, achieved by considerably lowered fuel consumption, can be generated in a highly systematic manner. We present a design framework capable of methodologically producing sets of planar transfers between two circular orbits as well as two elliptic orbits. In particular, it is shown that orbit transfers, consistent with planar dynamical systems of four bodies modeling the Jovian system, can be directly identified without differential corrections, and provide solutions with a significantly lower propulsion cost than the conventional Hohmann transfer.

Nomenclature

D	=	distance between the larger body and the smaller body, km or distance units (DU)
e, $\boldsymbol{e}$	=	orbital eccentricity and eccentricity vector
h	=	specific angular momentum, km^2/s
$IC-$, $IC+$	=	states of spacecraft before and after firing thrusters
M	=	mass, kg
R, r	=	distance between the body and the spacecraft in rotating and pulsating frames, km or DU
T	=	time, s or time units (TU)
U^*, u^*	=	effective potential functions in rotating and pulsating frame coordinates, km^2/s^2 or DU^2/TU^2
V_X, V_Y	=	X- and Y-direction velocity in rotating frame, km/s or DU/TU
${}^iV_X$, ${}^iV_Y$	=	${}^iX$- and ${}^iY$-direction velocity in inertial frame, km/s or DU/TU
ν, η	=	mass parameters for two-body and four-body systems
X, Y	=	rotating frame coordinates, km or DU
${}^iX$, ${}^iY$	=	inertial frame coordinates, km or DU
x, y	=	pulsating frame coordinates, km or DU
θ	=	true anomaly, rad
ϕ	=	angle between two eccentricity vectors, rad
ω	=	angular velocity, rad/s

Introduction

A METHODOLOGICAL procedure of finding planar impulsive transfers among planetary moons is demonstrated in this paper. For the problem formulation, a patched three-body approach is adopted, where a dynamical model representing a planetary system is decomposed into a series of perturbed three-body problems. A key idea of constructing transfers is then the use of a transportation tube network,[1,2] structured by the combination of orbital bundles of transit trajectories in the decomposed systems. The primary objective of this paper is to show that, through the transit orbit search algorithm developed in Yamato and Spencer,[3] sets of impulsive transfers between two circular orbits as well as two elliptic orbits in planar restricted problems of four bodies are identified without using differential corrections.

The intensive analysis on the phase space geometry of the circular restricted three-body problem (CR3BP) produced the important concept of a transportation tube network.[1,2] In the CR3BP phase space of rotating frame coordinates, there exist time-invariant manifolds[4,5] asymptotic to libration point ($L1$ and $L2$) periodic orbits.[6,7] The invariant manifolds of libration point orbits, consisting of continuously distributed asymptotic solutions, appear as distorted tubes in the CR3BP phase space. Based on the previous works by Conley,[8] McGehee,[9] and Llibre et al.,[10] the comprehensive study on such orbital structure was given by Koon et al.[11] The remarkable feature is that these manifold tubes enwrap an infinite number of solution trajectories, which are all going to encounter with the smaller primary forward or backward in time. The bundles of these orbits (called transit orbits because they involve a transit of regions, e.g., from the exterior to the smaller primary regions) can then serve for transportation passageways in the CR3BP phase space.

The transportation passageways,[1,2] formed by such transit orbits and guided by manifold tubes of libration point orbits, can offer numerous applications. For instance, the manifold structure in the CR3BP can provide an essential understanding of the dynamical behavior of comets beyond the two-body dynamics. In Koon et al.,[12] Howell et al.,[13] and Ross,[14] the validity of the CR3BP formalization was theoretically and numerically confirmed with some actually observed astronomical phenomena in the solar system, including resonant transitions of the Jupiter comets, Oterma or Gehrels 3, and a series of impacts of the fractured comet, Shoemaker-Levy 9, on Jupiter.

Another significant outcome provided by the transportation mechanics in the CR3BP phase space is an application to spacecraft trajectory design problems.[15–20] Based on the understanding of the CR3BP orbital structure, Koon et al.[11] theoretically proved the existence of solution orbits for any physically feasible sequence of regional transitions and developed a numerical procedure of systematically generating trajectories with the regional itinerary prescribed in advance. Through the design concepts, namely, Petit Grand Tour[15,16] and Shoot the Moon[17]; furthermore, it was shown that the produced impulsive transfers were featured by large savings of fuel consumptions in term of the velocity change when compared with the traditional Hohmann transfer. As also pointed out by other

Received 12 August 2003; revision received 24 February 2004; accepted for publication 24 February 2004.

*Ph.D. Student, Department of Aerospace Engineering; currently Research Engineer, Future Robotics Technology Center, Chiba Institute of Technology, Chiba 275-0016, Japan; yamato@furo.org. Member AIAA.

†Assistant Professor, Department of Aerospace Engineering, 229 Hammond Building; dbs9@psu.edu. Associate Fellow AIAA.

authors,[18–20] the multibody system approach beyond two-body dynamics enables one to generate fuel-effective impulsive transfers. The CR3BP formulation can offer an effective means to designing spacecraft trajectories.

With the presence of perturbing forces, although transit trajectory bundles, originally existing inside manifold tubes of libration point orbits in the ideal CR3BP phase space, change their distributions, they can persist for a long time and still remain as bundles, serving transportation passageways in the perturbed CR3BP system. A contribution in the previous work[3] is on the development of a systematic procedure of numerically identifying such transportation passageways under the influence of perturbing forces. As demonstrated, for instance, transportation tubes formed by perturbed transit orbits can be numerically and directly identified without using differential corrections in the CR3BP with multiple perturbing bodies, such as the circular restricted six-body problem with the sun.

One feature in the design framework presented here is the elimination of the need for differential corrections from the transfer design within planar restricted problems of four bodies. In the literature on transfer designs such as the two-body formulation, for example, the sequence of orbital arcs, constructed by designing short mission orbits in the decomposed systems, must be differentially corrected via numerical iterations (called differential corrections, e.g., shooting methods). Because of the high sensitivity, the convergence of these iterative processes is usually hard even for the system of a relatively small number of celestial bodies (e.g., the inclusion of the first perturbing body has a greater impact than the second perturbing body inclusion). Although differential corrections or some targeting schemes are still required in considering the consistency with the ephemeris model and the specification of some additional transfer properties, the methodology established in this paper can produce numerous impulsive transfers directly in planar restricted models of four bodies without using differential correction processes.

Referred to as a miniature solar system, the Jovian system, consisting of the gas giant and its numerous natural moons, has recently been attracting much attention of researchers in space science. As applications of the space trajectory design, planar impulsive transfers among the Jupiter moons, more specifically starting from a parking orbit around Ganymede and ending at a parking orbit around Europa, are examined. In the first example, under a simplifying assumption that both of the Jovian satellites are on circular orbits centered at Jupiter in the same orbital plane, planar transfers between these circular orbits are identified. Subsequently, the assumption is generalized, so that transfers between two elliptic orbits in the same orbital plane can be achieved. It is shown that for both cases entire transfers consistent with the planar dynamical models of four bodies in the inertial frame can be systematically found without differential corrections. Additionally, the total propellant is successfully reduced in contrast with the standard Hohmann transfer, and the transfer time is reasonable.

Model Decomposition

The methodology of the model decomposition is first discussed. Planar orbit transfers among planetary moons by impulsive maneuvers are the primary application addressed in this paper. At the first stage in the design process, a preestablished planar dynamical system, modeling a planetary system in the inertial frame (referred to as a full dynamical model in this paper), is decomposed into a series of base models. The examples of the base models in this paper include the planar circular restricted four-body problem (CR4BP) and the planar elliptic restricted four-body problem (ER4BP). As will be shown later, these base models can be formulated as a planar CR3BP with perturbing forces. By the search method developed in Ref. 3, a preferable short mission orbit can be identified in each base model, and then, the resulting sequence of trajectory arcs is patched together in the full dynamical system of four bodies. In this paper, we use the term *full dynamical system* to represent the preestablished planar dynamical model, consisting of several celestial bodies (in particular, not for the ephemeris model).

In either the two- or three-body approaches, model decompositions usually involve reducing the number of celestial bodies. The truncation of celestial bodies is required to simplify the process of constructing mission orbits in the decomposed systems. However, the subsequent design step of patching, or continuing, the sequence of these identified orbital arcs in the full dynamical model becomes very challenging even for simplified systems. Although the sensitivity, inherently caused by the inverse-square gravitational field, can offer various trajectory options, it also renders numerical iterative processes, such as differential corrections, for which convergence is difficult.

One of the key features in the presented design framework is the exclusion of such differential corrections from the design process within restricted four-body systems. In this study, without reducing the number of celestial bodies, an assumed planar full dynamical system of several celestial bodies is decomposed into a series of perturbed three-body systems. These base models are derived only through some coordinate transformations and unit normalizations. A general assumption adopted for the targeted full dynamical system is that all of the celestial bodies are orbiting in the same plane. Consequently, all of the celestial bodies in any base systems, formulated only by coordinate transformations and unit normalizations, are also in the same orbital plane.

Equations of Motion for Base Systems

Before addressing the demonstration of the new design framework, mathematical models for the base systems are briefly described. These base models are formulated as a CR3BP with perturbations caused by the fourth body and the eccentricity. For the discussion about the equations of motion for the CR3BP, refer to Szebehely.[21]

Planar Circular Restricted Four-Body Problem: CR4BP

A mathematical model, namely, the planar circular restricted four-body problem (CR4BP), is described here. This model consists of a space vehicle, a larger mass M_1, and two smaller masses M_j with $j = 2, 3$. It is assumed that both of the smaller bodies are circulating around M_1 with the constant radii D_j and angular velocities ω_j, forming concentric circles on the same plane as shown in Fig. 1.

In this model, the origin of the inertial frame is at the body M_1, and the ${}^iX{}^iY$-plane coincides with the orbital plane. Similar to the usual CR3BP model, the rotating frame is introduced, where the X axis is fixed on the circulation of the targeted body M_2, with the origin at the body M_1, and the Y axis is on the orbital plane. The equations of motion are scaled with the radius D_2, the angular velocity ω_2, and the sum of the first and the second bodies $M_1 + M_2$.

The motion of the infinitesimal small body under this gravitational field is expressed by

$$\ddot{X} - 2\dot{Y} = U_X^*, \qquad \ddot{Y} + 2\dot{X} = U_Y^* \tag{1}$$

where

$$U^* = (X^2 + Y^2)/2 + \eta_1/R_1 + \eta_2/R_2 + \eta_3/R_3$$

$$\eta_j = M_j/(M_1 + M_2)$$

$$R_1 = \{X^2 + Y^2\}^{\frac{1}{2}}, \qquad R_2 = \{(X-1)^2 + Y^2\}^{\frac{1}{2}}$$

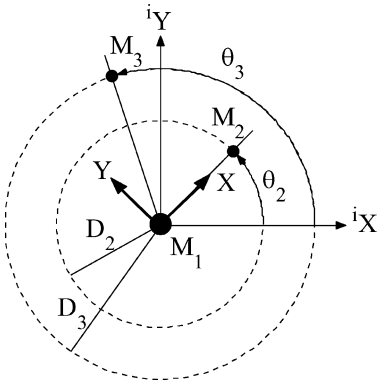

Fig. 1 Geometry of planar CR4BP.

$$R_3 = \left\{ \left[X - (D_3/D_2)\cos(\theta_3 - \theta_2) \right]^2 + \left[Y - (D_3/D_2)\sin(\theta_3 - \theta_2) \right]^2 \right\}^{\frac{1}{2}}, \qquad \theta_j = \omega_j T + \theta_{j0}$$

In these equations, the subscripts, X and Y, attached to U^* denote the partial derivatives with respect to X and Y, respectively, and η_j for $j = 1, 2, 3$ are the normalized mass parameters. The rotating frame is attached to the circulation of the body M_2 in this expression. With the appropriate change of the radii D_j, however, the rotating frame can be easily switched to the motion of the body M_3.

There are two differences between the nominal CR3BP and this CR4BP models. One is the additional gravitational force caused by the fourth celestial body, represented by an additional term in the effective potential function U^*. The second is caused by the different location of the rotational center. In the CR3BP model, two primaries are circulating around their barycenter, whereas the rotational center of the smaller bodies in the CR4BP is located at the larger body. This discrepancy should be also considered as a part of the perturbations.

Planar Elliptic Restricted Four-Body Problem: ER4BP

Another dynamical model introduced here for the base model is the planar elliptic restricted four-body problem (ER4BP). As illustrated in Fig. 2, there are three celestial bodies in the same orbital plane, that is, a larger body M_1 and two smaller bodies M_j with $j = 2, 3$. The smaller bodies are assumed to be on elliptic orbits with the focus at the body M_1 and with different eccentricity vectors $\boldsymbol{e}_2$ and $\boldsymbol{e}_3$.

The origin of the inertial frame is attached at the body M_1, the positive ${}^iX$ axis coincides with the eccentricity vector of the body M_2, and the ${}^iY$ axis is on the orbital plane. Similar to the CR4BP model, the positive X axis of the rotating frame is fixed on the circulation of the body M_2 with the origin at the body M_1.

After transforming the equations of motion from the inertial frame to the rotating frame, and subsequently applying the pulsating coordinates,[22] defined on the elliptic motion of the body M_2,

$$X = D_2(\theta_2)x, \qquad Y = D_2(\theta_2)y \tag{2}$$

the ER4BP model takes the form

$$x'' - 2y' = u^*_x + \varepsilon(\theta_2)u^*_x, \qquad y'' + 2x' = u^*_y + \varepsilon(\theta_2)u^*_y \tag{3}$$

where

$$u^* = \frac{x^2 + y^2}{2} + \frac{\eta_1}{r_1} + \frac{\eta_2}{r_2} + \frac{\eta_3}{r_3}, \qquad \eta_j = \frac{M_j}{M_1 + M_2}$$

$$\varepsilon(\theta_2) = \frac{-e_2\cos\theta_2}{1 + e_2\cos\theta_2}$$

$$r_1 = \{x^2 + y^2\}^{\frac{1}{2}}, \qquad r_2 = \{(x-1)^2 + y^2\}^{\frac{1}{2}}$$

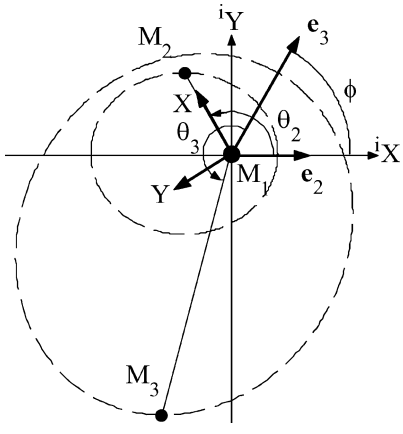

Fig. 2 Geometry of planar ER4BP.

$$r_3 = \left\{ \left[x\cos\theta_2 - y\sin\theta_2 - \frac{D_3}{D_2}\cos(\theta_3 + \phi) \right]^2 + \left[x\sin\theta_2 + y\cos\theta_2 - \frac{D_3}{D_2}\sin(\theta_3 + \phi) \right]^2 \right\}^{\frac{1}{2}}$$

$$D_j = \frac{h_j^2/\nu_j}{1 + e_j\cos\theta_j}$$

In this expression, r_j and D_j denote the distances from the body M_j to the spacecraft and from the larger body M_1 to the body M_j, respectively; h_j and e_j represent the specific angular momentum and the eccentricity of the body M_j, ν_j is a mass parameter defined by $\nu_j = G(M_1 + M_j)$, and the subscriptions x and y, attached to the effective potential function u^*, represent the partial derivative with respect to x and y. The prime indicates the derivative with respect to the true anomaly of the body M_2. Note that in each time step of numerical integration of the ER4BP, a root finding iteration such as the Newton method is required to determine true anomalies of the smaller primaries θ_2 and θ_3. The dynamical system in Eq. (3) can be viewed as a CR3BP with perturbations caused by the fourth body and the eccentricity.

Transportation-Tube Network

Central to the development of the transfer design framework is the use of the transportation-tube network.[1,2] The transportation tube is, in this paper, considered to be formed by bundles of perturbed transit orbits, which originally exist inside invariant manifolds of libration point orbits in the CR3BP.

Phase Space Structure of CR3BP

In Fig. 3, global and local structures of unstable and stable manifolds of libration point orbits in the Jupiter–Europa CR3BP system are reproduced (originally presented in Koon et al.[11]). The collections of the black and gray curves indicate unstable and stable manifolds, respectively. In this paper, an invariant manifold of a libration point orbit is referred to as an invariant surface in the phase space, formed by continuously distributed solution orbits asymptotic to the libration point orbit. Although there are other time-invariant manifolds, such as equilibrium points or periodic orbits, we refer to invariant manifolds only as those asymptotic to libration point orbits in this paper for a distinction. Wiggins[4] and Perko[5] include additional mathematical descriptions about manifolds for general dynamical systems.

The important feature of the CR3BP orbital structure is that the inside of these manifold tubes are filled up only with so-called transit orbits,[11] that is, solution orbits transiting from one region to another through the $L1$ or $L2$ periodic orbit. In Fig. 3b, an example of transit trajectory from the exterior to the second primary regions is schematically illustrated. Note that although only the projections onto the configuration space are shown in the figure (approximately 40 asymptotic orbits for each manifold), the unstable and stable manifolds are considered as distorted and squashed tubular surfaces in the phase space.

The transportation passageways are formed by these bundles of transit orbits. As shown in Fig. 3a, two sets of unstable and stable manifolds emanate from the vicinity of the second primary toward the exterior and the interior regions. (In Fig. 3b, only the manifolds associated with an $L2$ periodic orbit are presented.) In the inertial frame, hence, these four manifold tubes in the exterior and the interior regions accompany the smaller primary, orbiting around the lager primary. Under the influence of other perturbing bodies, although the transit orbit bundles inside these manifold tubes are deformed, they can remain still as bundles for a considerable time, serving as transportation passageways. It can be expected that in the solar system many celestial bodies, such as planets or natural satellites, circulating around the sun or a planet, trail these transportation passageways.

Two clarifications of the terminology used in this paper are made. First, manifolds of libration point orbits in the CR3BP are precisely

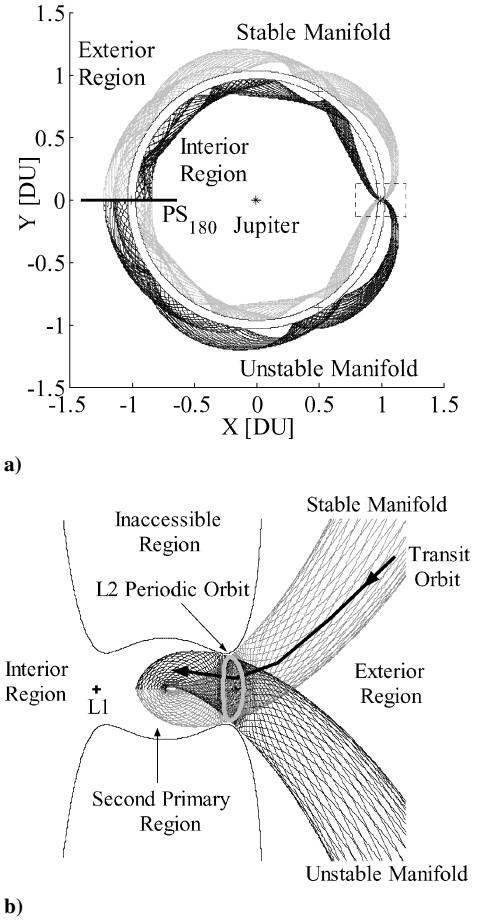

Fig. 3 Structures of unstable and stable manifolds in the Jupiter–Europa CR3BP system[11]: a) global and b) local.

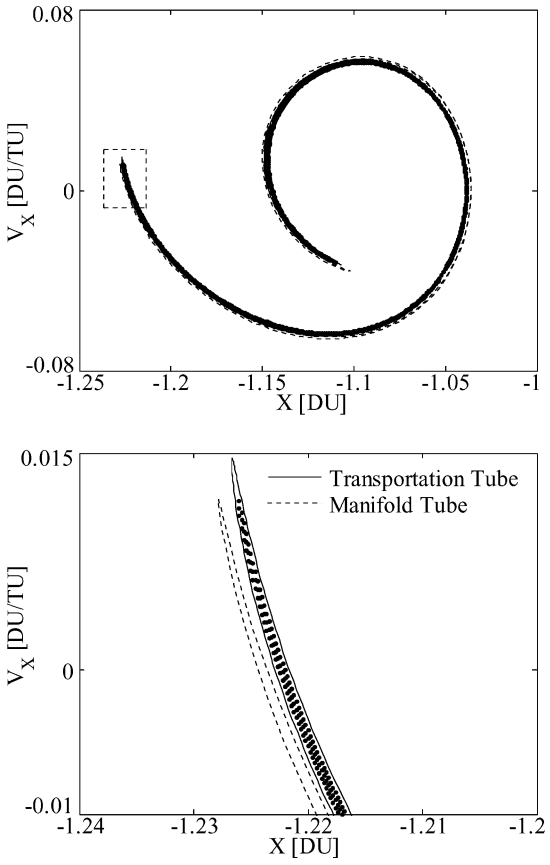

Fig. 4 Results of transit orbit search in the planar CR6BPS.[3]

defined in mathematical terms based on the existence and the hyperbolic nature of periodic orbits around libration points. We cannot in general expect the existence of time-invariant manifolds in the CR3BP with time-depending perturbations. In the remaining part of the paper, we refer to the term transportation passageways as bundles of transit orbits only for the perturbed CR3BP systems. Second, in Fig. 3a, a Poincaré section labeled by PS_{180} is also depicted by a solid line at $X < 0$ and $Y = 0$. In this paper, Poincaré section is a surface of section defined at an arbitrarily location in the phase space, where solution orbits crossing transversally that section are studied. We refer to the term Poincaré cut as an intersection between the manifold (or transportation) tube and the Poincaré section. Although this term is not a precise technical term in applied mathematics, we frequently use the word Poincaré cut to express their intersection for convenience.

The numerical method of computing manifold and transportation tubes are briefly described. In the ideal CR3BP, unstable (or stable) manifold trajectories asymptotic to libration point orbits can be numerically generated by repeatedly integrating the CR3BP model forward (or backward) in time. A set of initial values for these numerical integrations are obtained along libration point orbits thorough linear approximations of unstable (or stable) subspaces using eigenvectors of monodolomy matrix.[6,7,23,24] The globalization of manifolds is then terminated if the spacecraft reaches the specified Poincaré section. Similar to the ideal CR3BP case, transportation tubes in perturbed CR3BP systems are numerically generated by simply integrating the full dynamical system including perturbations, starting from the same set of the initial values as those for the manifold tube computation. The transit orbit search is then performed inside the resulting Poincaré cut of transportation tubes. The detailed discussions of the transportation tube computation and the transit orbit search procedure for perturbed CR3BP systems are found in Ref. 3.

Transit Orbit Search Example

A key feature in the transit orbit search procedure developed in Ref. 3 is that perturbed transit orbits can be found uniformly inside the Poincaré cut of transportation tubes. An example result of the transit orbit search is shown in Fig. 4 (extracted from Ref. 3) for the circular restricted six-body problem with the Sun (CR6BPS). This model consists of Jupiter, four Galilean satellites and the sun, and in addition to their gravitation forces, the circulation of the Jovian system around the sun is also taken into account. Similar to the CR4BP, the CR6BPS is formulated on the rotating frame fixed on the circulation of the targeted body Europa and centered at the first primary Jupiter, resulting in a Jupiter–Europa CR3BP system under multiple perturbation sources. The Poincaré section in this example is defined at $X < 0$ and $Y = 0$ similar to Fig. 3a. In Fig. 4, the Poincaré cuts of the exterior stable transportation and manifold tubes are projected on the $X - V_X$ plane, and represented by the solid and the dashed closed curves, respectively. Each dot indicates a state of transit orbits found through the search procedure on this Poincaré section.

As seen in Fig. 4, a transportation tube drifts from the original location of the exterior stable manifold tube caused by the perturbations and a large number of transit orbits, crossing transversally the Poincaré section, are uniformly found inside the transportation-tube cut. We remark that the search method developed in Ref. 3 can identify transit orbit bundles successfully in planar circular restricted problems of multiple bodies, where all of the celestial bodies are on their circular orbits in the same plane. In this paper, however, we only discuss the procedure of finding orbit transfers in the planar restricted problems of four bodies.

Outline of Design Process

Next, we outline the entire design process. Although the transfer design problem between two concentric circular orbits is mainly addressed here for demonstration purposes, the process described can be applied to the transfer design problem between two elliptic orbits.

Model Decomposition

At the first stage, the planar full-body dynamical model in the inertial frame, consisting of four bodies, that is, Jupiter, Europa, Ganymede, and spacecraft, is decomposed into two CR4BP models listed in Table 1 (for transfers between two circular orbits). Both of these models can be interpreted as an ideal planar three-body system with perturbing forces. Note that two planar ER4BP systems will be employed later as base models to construct a transfer between two elliptic orbits.

As stated earlier, the model decomposition usually involves the truncation of the number of celestial bodies. In this paper, however, the decomposition means merely establishing a few base models (two models here) by normalizing the full model of four bodies on some rotating frames. All of the celestial bodies in the original full-body system are thus included in the base models.

Transportation-Tube Construction and Dynamical Channel Search

Combining transportation tubes of the base models provides the intersatellite transportation network. For each of the base systems, a transportation tube is numerically constructed, and their intersection in the position space is located. As an example, the unstable and stable transportation tubes are constructed and superimposed on the rotating frame of the Europa system in Fig. 5.

The entire transfer consists of two parts, namely, a departure orbit from Ganymede and an arrival orbit at Europa. As shown in Fig. 5, an unstable interior transportation tube in the Ganymede system and a stable exterior transportation tube in the Europa system are employed to search the departure and the arrival orbits, respectively.

It should be emphasized here that the word *intersection* is used for representing an intersection of two transportation tubes in the position space, not in the phase space. At the intersection, thus, the transfer orbits inside these two transportation tubes are continuous in terms of the position and discontinuous in terms of the velocity. Firing thrusters at the intersection, hence, makes it possible to jump from one transportation tube to another (tube jumping).

Transit Orbit Search

In each base system, a bundle of perturbed transit orbits can systematically be identified inside the transportation tube cut as presented in Fig. 4. Once the intersection in the configuration space is located, a number of transfers from Ganymede to Europa can be systematically found inside the intersecting region of the transportation tunnels.

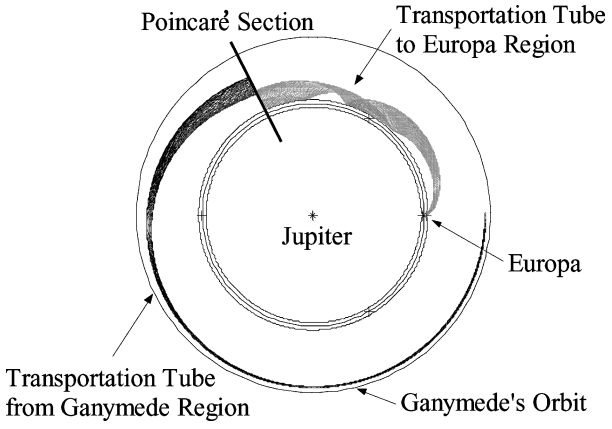

Fig. 5 Departure and arrival transportation tunnels.

Similar to the methodology developed by Koon et al.,[15,17] two sets of states on the intersection are identified at this design step. These two sets of the states are such that if the Europa system is numerically integrated from one of the sets forward in time the spacecraft is going to encounter with Europa, and if the Ganymede system is numerically integrated from the other set backward in time the spacecraft is going to encounter with Ganymede. Furthermore, these two sets are continuous in the position space as mentioned before.

End-to-End Transfer via Transportation Tube Jumping

The identified transit orbits, that is, states on the Poincaré section yielding transit orbits, are transformed back to the inertial frame coordinates, and the dynamical model in the inertial frame is numerically integrated with those initial states to produce an end-to-end transfer. The velocity discontinuity between the identified states can then be used to determine the required ΔV. The feasibility is finally evaluated in terms of the ΔV and the transfer time. Note that velocity changes required to depart from and to arrive at parking orbits around the targeted bodies are ignored in this evaluation.

Astronomical Constants

The astronomical constants used in the design demonstrations are summarized in Table 2. These values are taken from Dunham and muhonen.[25] Note that the normalized distant and time units denoted by DU and TU are equal to the semimajor axis and the inverse of the mean motion, respectively. The values of the mean motion are calculated from the *GM* and the semimajor axis listed in Table 2.

In the transfer design example between two elliptic orbits, $\phi = 2.8841$ rad is used for the angle between the two eccentricity vectors. This value is calculated from the ephemeris data (data available online at http://www.imcce.fr [cited 3 October 2002]) on 1 January 2003 by projecting the eccentricity vectors onto the X–Y plane. Note that in this paper planar impulsive transfers are concerned, and two elliptic orbits of Europa and Ganymede are assumed to be on the same orbital plane with the focus at Jupiter.

Numerical Integration

For the numerical construction of transportation tubes and transfer orbits, we use a fourth-order one-step explicit numerical integrator (Runge–Kutta type) with the step size control technique, provided in MATLAB®. In the transfer orbit design, the relative and the absolute error tolerances are set to 10^{-10} and 10^{-12} (corresponding to less than 1 m), respectively. Note that numerical integrators, provided in MATLAB, feature an event detection function. For the Poincaré cut construction, that is, the computation of an intersection between the specified Poincaré section and the transportation (or manifold) tube, for instance, this feature enables one to terminate numerical integrations automatically when the spacecraft reaches the section specified in advance. The computation time in MATLAB can be remarkably reduced if the dynamical equations are provided by so-called Mex files (written in C-Language).

Table 2 Astronomical constants for Europa and Ganymede systems[25]

Parameter	Jupiter	Europa	Ganymede
GM, km^3/s^2	126,712,767.000	3,202.721	9,887.830
Semimajor axis, km	——	671,000	1,070,000
Eccentricity	——	0.009	0.002

Table 1 Definition of planar CR4BP models

Base model	Model definition
Ganymede system	Jupiter–Ganymede spacecraft circular three-body system with a perturbing body Europa on an inner circular orbit
Europa system	Jupiter–Europa spacecraft circular three-body system with a perturbing body Ganymede on an exterior circular orbit

Orbit Transfers in Planar Circular Restricted Four-Body Problem

In this section, the design process of transfers between two circular orbits is demonstrated. Similar to Koon et al.,[15] it is assumed that when the spacecraft fires its thrusters for the transit from the unstable to the stable transportation tubes all of the bodies, spacecraft, Jupiter, Europa, and Ganymede, are aligned on the ${}^iX$ axis. In Figs. 6 and 7, the Poincaré cuts of the unstable and stable transportation tunnels, that is, intersections between transportation tubes and the Poincaré section defined by $X < 0$ and $Y = 0$ are projected on the $X - V_X$ and $X - V_Y$ planes.

In the figures, the solid and the dotted closed curves represent the transportation and the manifold tube cuts, respectively, and the Poincaré cuts of the departure transportation tube in the Ganymede system are transformed into the Europa's rotating coordinates and superimposed onto the Poincaré cut of the Europa's arrival transportation tube. To affect the impulsive transfer, or more specifically the jumping from the unstable to the stable transportation tubes, the continuity in terms of the position is required. As is clear from the figures, these tube cuts have an intersection in the configuration space roughly from $X = -1.23$ DU to $X = -1.22$ DU (and $Y = 0$ DU). Because inside each closed curve transit orbits can be uniformly identified as seen in Fig. 4, the orbit transfers from Ganymede to Europa regions are found for any locations in the intersection region.

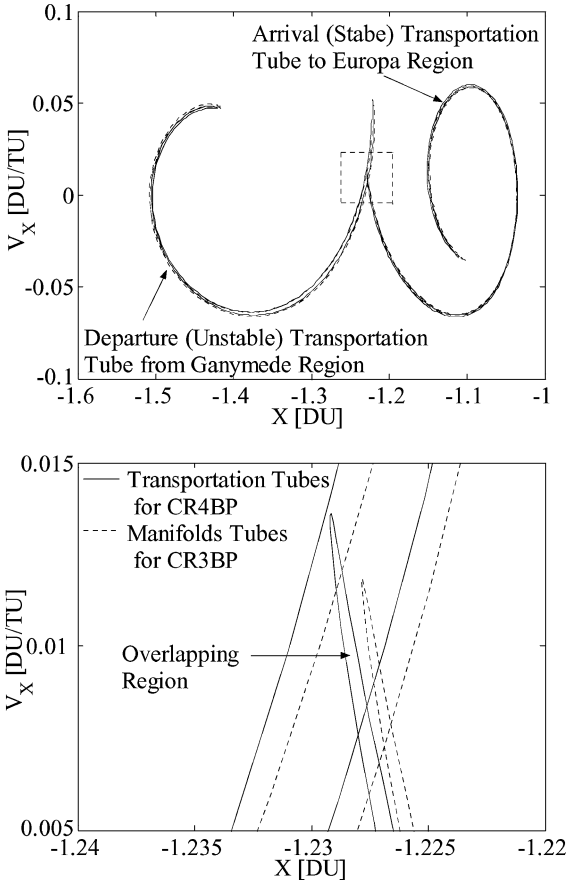

Fig. 6 $X - V_X$ projection of the intersections between Poincaré section and (departure and arrival) transportation tubes.

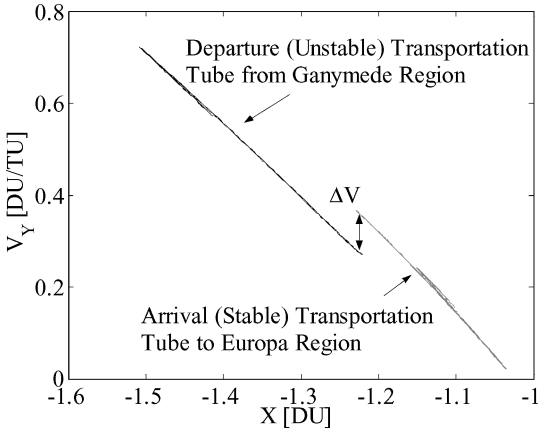

Fig. 7 $X - V_Y$ projection of the intersections between Poincaré section and (departure and arrival) transportation tubes.

As is also clear from Fig. 6, these transportation tubes have an overlapping region on the $X - V_X$ projection. For any selected location inside the overlapping area, therefore, it is possible to specify a pair of states, which are also continuous in terms of the V_X velocity, resulting in the impulsive transfers by a tangential firing in this example. It is, however, more advantageous to use separately the V_X velocity, so that each of the transit orbits, that is, departure and arrival orbits, could have some desired properties, such as departure and arrival altitudes.

Note that as indicated in Figs. 6 and 7, the magnitude of the V_Y velocity is much greater than the magnitude of the V_X velocity in this Poincaré section. The total amount of the ΔV required for the tube jumping is consequently dominated by the discontinuity of the V_Y velocity, as represented by ΔV in Fig. 7. Although the magnitude of the V_Y discontinuity is very similar along the intersecting region (from $X = -1.23$ to -1.22 DU), the fuel effective transfer evaluated by ΔV can be found by simply selecting a patching point, where the smallest magnitude of the discontinuity in terms of the V_Y velocity is achieved. Note, too, that the intersecting region of these transportation tubes in the position space is spread over roughly 6710 km ($= 0.01$ DU) along the negative X axis.

An example of the entire transfers from Ganymede to Europa is plotted in Fig. 8. For simplicity, we assume that when the spacecraft is at the patching point on the negative ${}^iX$ axis Europa and Ganymede are both situated on the positive X axis. The states of the spacecraft at the patching point in the inertial coordinates are listed in Table 3. Note that $IC-$ (or $IC+$) indicates a state before (or after) firing thrusters, and if the full four-body dynamical system in the inertial frame is numerically integrated from $IC-$ (or $IC+$) backward (or forward) in time the spacecraft is going to enter the region of Ganymede (or Europa).

In this example, the thruster must be fired at the marked location, amounting approximately $\Delta V = 1174$ m/s in order to jump up from the departure to the arrival tubes, and the transfer time is roughly 28 days. Note that 2822 m/s and three days are necessary for a Hohmann transfer. Although the transfer time increased 10-fold,

Table 3 States of spacecraft before and after firing thrusters (CR4BP)

States	${}^iX$, km	${}^iY$, km	${}^iV_X$, km/s	${}^iV_Y$, km/s
$IC-$	−823,988.00	0.0	0.15107142	−13.02847653
$IC+$	−823,988.00	0.0	0.12944601	−11.85535506

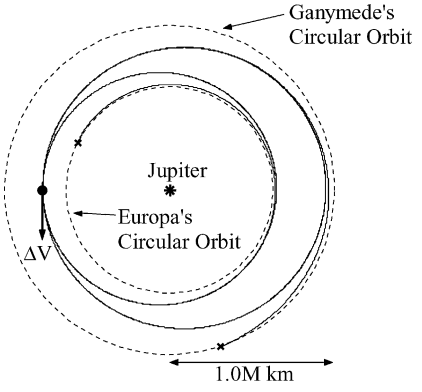

Fig. 8 Example transfer between two circular orbits.

the ΔV required for the transfer is considerably reduced (less than half).

In Figs. 9a and 9b, the departure and the arrival phases are enlarged in the rotating frames. The transfer starts from the circular orbit with the altitude of 289 km above Ganymede and completes at the circular orbit with the altitude of 212 km above Europa. These altitudes are obtained through the arbitrarily selections of different magnitudes of the V_X velocity on the Poincaré section.

Any physical location inside the intersecting region (roughly from $X = -1.23$ DU to $X = -1.22$ DU and $Y = 0$ DU) shown in Fig. 6 can produce a number of transfer orbits, and slight variations of the V_X velocity can provide transit orbits with various properties. It should be also emphasized that although differential corrections are not required to find such numerous impulsive transfers differential corrections can be applied on these identified set of transfers in order to enforce additional transfer properties, such as departure and arrival altitudes.

Orbit Transfers in Planar Elliptic Restricted Four-Body Problem

As a more practical application, the design procedure discussed so far is applied to the transfer design problem between two elliptic orbits. To make a transfer from Ganymede to Europa, an interior unstable transportation tube of Ganymede and an exterior stable transportation tube of Europa must intersect in the configuration space. Fortunately, the intersection of these transportation tunnels exists, and it can be located without difficulty.

Similar to the earlier transfer design problem, once the intersecting region is found, a set of transit orbits on each ER4BP system is easily determined by the transit orbit search procedure. In Ref. 3, the numerical procedure of finding transportation passageways is demonstrated only on the Jupiter–Europa planar elliptic three-body system with the perturbing body, Ganymede. The exact same process with backward time can be applied to the Jupiter–Ganymede planar elliptic three-body system with the perturbing body, Europa, in order to identify a departure transportation tube.

In the usual manner, the differential correction must be employed to generate an entire transfer consistent with the original elliptical restricted system of four bodies. However, only the coordinate transformation back to the inertial frame is required because the departure and the arrival transfer orbits determined in the decomposed base models are already solutions of the dynamical system of four bodies including the eccentricity effects.

An entire impulsive transfer from the vicinity of Ganymede to the vicinity of Europa is plotted in Fig. 10. In this example, the true anomalies of Europa and Ganymede are $\theta_2 = -20$ deg and $\theta_3 = -30$ deg when the spacecraft is at the transiting point. The states of spacecraft before and after firing the thrusters in the inertial frame, namely, $IC-$ and $IC+$, are listed in Table 4. Note that if the ER4BP in the inertial frame is numerically integrated from $IC-$ (or $IC+$) backward (or forward) in time, the spacecraft is going to enter the region of Ganymede (or Europa) and encounter with the second body.

To achieve the jumping between the transportation tunnels, that is, from the unstable tube of the Ganymede system to the stable tube of the Europa system, $\Delta V = 1387$ m/s is required at the marked location. The transfer time is roughly 25 days in this example. As summarized in Table 5, the amount of the ΔV is considerably reduced by elongating the transfer time in contrast with the traditional

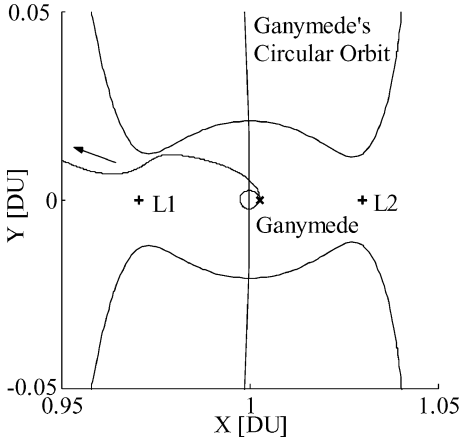

Fig. 9a Departure of transfer in rotating frames.

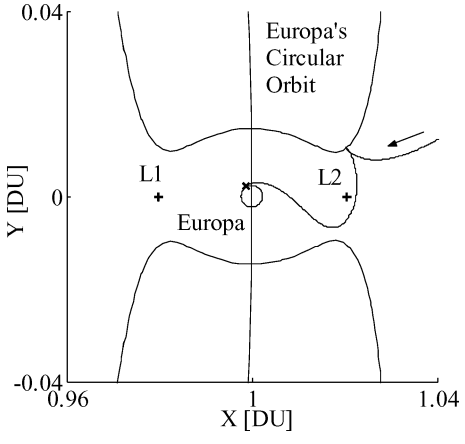

Fig. 9b Arrival of transfer in rotating frames.

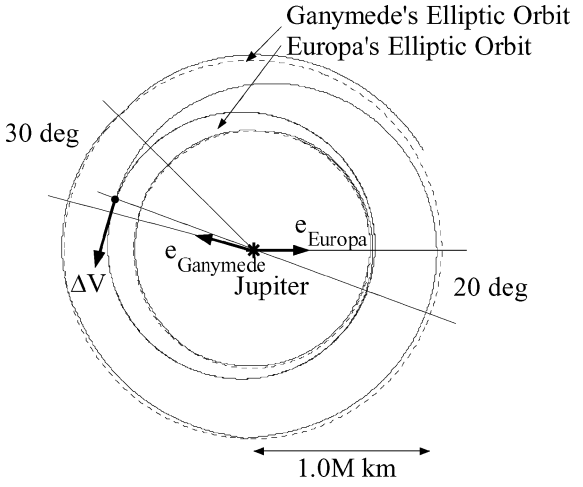

Fig. 10 Example transfer between two elliptic orbits.

Table 5 Summary of transfer characteristics

Transfer characteristic	Hohmann transfer	Transfer between two circular orbits	Transfer between two elliptic orbits
Velocity change, m/s	2822	1174	1387
Transfer time, days	3	28	25

Table 4 States of spacecraft before and after firing thrusters (ER4BP)

State	${}^iX$, km	${}^iY$, km	${}^iV_X$, km/s	${}^iV_Y$, km/s
$IC-$	−778,368.09001162	283,302.81606686	−3.68482159	−0.12.41310344
$IC+$	−778,368.09001162	283,302.81606686	−4.02838459	−0.1106896243

Hohmann transfer, similar to the preceding transfer problem. The transfer time can still be considered as reasonable.

Conclusions

The main feature of the presented framework is that a number of impulsive transfers with significant velocity-change advantages (when compared with the traditional Hohmann transfer) can be identified in planar restricted problems of four bodies without differential corrections. In the literature, it is required to numerically and iteratively correct the sequence of orbit arcs in order to gain the consistency even with the simplified model. In this sense, the developed approach can be completely distinguished from the existing methodologies.

One of the strong requirements to achieve successful impulsive transfers through this framework is the existence of an intersection of transportation tubes in the configuration space. The discontinuity in terms of the velocity among transportation tubes can be overcome by firing thrusters. However, the continuity in the position space is indispensable to make transits between two transportation tubes feasible. If it is infeasible to jump up directly from one transportation tunnel to another because of the nonexistence of their intersection, some additional maneuver techniques connecting two transportation tunnels are required.

The methodology of this paper is limited only to the problem of finding transfers in planar restricted systems. Gómez et al.[16] showed that the invariant manifolds asymptotic to libration point orbits in the spatial CR3BP also act as separatrix as seen in the phase space of the planar CR3BP, and also presented that the similar technique to the planar CR3BP can be applied for the spatial CR3BP by adequately using additional dimensionalities as design parameters. An extension of the presented methodology to the spatial CR3BP system with perturbations is a future work.

Another issue addressed as a long-term future work is to develop a design algorithm capable of generating flight-ready spacecraft trajectories directly using a real-world ephemeris model. The overall structure of transit orbits bundles in the CR3BP phase space is generally preserved from the influence of perturbations (although any small perturbation has a crucial effect on a specific orbit). We can expect that bundles of transit orbits exist still as bundles somehow in the complete ephemeris model and in the real solar system. A methodology of identifying transportation tubes in the ephemeris model can have a great impact on trajectory design problems.

Acknowledgments

The topic in this paper is a part of the conference paper presented at the 13th Space Flight Mechanics Meeting, Ponce, Puerto Rico, and was selected to receive a John V. Breakwell Student Travel Award. The authors express our gratefulness to the Breakwell award subcommittee for the award and Martin W. Lo from the Jet Propulsion Laboratory for the early discussions on this topic.

References

[1]Lo, M. W., and Ross, S. D., "The Lunar L1 Gateway: Portal to the Stars and Beyond," AIAA Paper 2001-4768, Aug. 2001.

[2]Lo, M. W., and Ross, S. D., "Low Energy Interplanetary Transfers Using The Invariant Manifolds of L1, L2 and Halo Orbits," American Astronautical Society, Paper: 98-136, Feb. 1998.

[3]Yamato, H., and Spencer, D. B., "Transit-Orbit Search for Planar Restricted Three-Body Problems with Perturbations," *Journal of Guidance, Control, and Dynamics*, Vol. 27, No. 6, 2004, pp. 1035–1045.

[4]Wiggins, S., *Introduction to Applied Nonlinear Dynamical Systems and Chaos*, Springer-Verlag, New York, 1990.

[5]Perko, L., *Differential Equations and Dynamical Systems*, 3rd ed., Springer-Verlag, New York, 2000.

[6]Barden, B. T., "Using Stable Manifolds to Generate Transfers in the Circular Restricted Problem of Three Bodies," M.S. Thesis, School of Aeronautics and Astronautics, Purdue Univ., West Lafayetta, IN, Dec. 1994.

[7]Howell, K. C., Barden, B. T., and Lo, M. W., "Application of Dynamical Systems Theory to Trajectory Design for a Libration Point Mission," *Journal of the Astronautical Sciences*, Vol. 45, No. 2, 1997, pp. 161–178.

[8]Conley, C., "Low Energy Transit Orbits in the Restricted Three-Body Problem," *SIAM Journal on Applied Mathematics*, Vol. 16, No. 4, 1968, pp. 732–746.

[9]McGehee, R. P., "Some Homoclinic Orbits for the Restricted Three–Body Problem," Ph.D. Dissertation, Dept. of Mathematics, Univ. of Wisconsin, Madison, WI, 1969.

[10]Llibre, J., Martinez, R., and Simó, C., "Transversality of the Invariant Manifolds Associated to the Lyapunov Family of Periodic Orbits near L2 in the Restricted Three-Body Problem," *Journal of Differential Equations*, Vol. 58, No. 1, 1985, pp. 104–156.

[11]Koon, W. S., Lo, M. W., Marsden, J. E., and Ross, S. D., "Heteroclinic Connections Between Periodic Orbits and Resonance Transitions in Celestial Mechanics," *Chaos*, Vol. 10, No. 2, 2000, pp. 427–469.

[12]Koon, W. S., Lo, M. W., Marsden, J. E., and Ross, S. D., "Resonance and Capture of Jupiter Comets," *Celestial Mechanics and Dynamical Astronomy*, Vol. 81, No. 1–2, 2001, pp. 27–38.

[13]Howell, K. C., Marchand, B. G., and Lo, M. W., "Temporary Satellite Capture of Short-Period Jupiter Family Comets from the Perspective of Dynamical Systems," *Journal of the Astronautical Sciences*, Vol. 49, No. 4, 2001, pp. 539–557.

[14]Ross, S. D., "Statistical Theory of Interior-Exterior Transition and Collision Probabilities for Minor Bodies in the Solar System," *International Conference on Libration Point Orbits and Applications, Girona, Spain*, World Scientific, River Edge, NJ, 2003.

[15]Koon, W. S., Lo, M. W., Marsden, J. E., and Ross, S. D., "Constructing a Low Energy Transfer Between Jovian Moons," *Contemporary Mathematics*, Vol. 292, 2002, pp. 129–145.

[16]Gómez, G., Koon, W. S., Lo, M. W., Marsden, J. E., Masdemont, J., and Ross, S. D., "Invariant Manifolds, the Spatial Three-Body Problem and Space Mission Design," American Astronautical Society, Paper 01-301, Aug. 2001.

[17]Koon, W. S., Lo, M. W., Marsden, J. E., and Ross, S. D., "Low Energy Transfer to the Moon," *Celestial Mechanics and Dynamical Astronomy*, Vol. 81, No. 1–2, 2001, pp. 63–73.

[18]Belbruno, E. A., and Miller, J. K., "Sun-Perturbed Earth-to-Moon Transfers with Ballistic Capture," *Journal of Guidance, Control, and Dynamics*, Vol. 16, No. 4, 1993, pp. 770–775.

[19]Lo, M. W., Williams, B. G., Bollman, W. E., Han, D., Hahn, Y., Bell, J. L., Hirst, E. A., Corwin, R. A., Hong, P. E., Howell, K. C., Barden, B., and Wilson, R., "Genesis Mission Design," *Journal of the Astronautical Sciences*, Vol. 49, No. 1, 2001, pp. 169–184.

[20]Villac, B. F., and Scheeres, D. J., "Escaping Trajectories in the Hill Three-Body Problem and Applications," *Journal of Guidance, Control, and Dynamics*, Vol. 26, No. 2. 2003, pp. 224–232.

[21]Szebehely, V. G., *Theory of Orbits: The Restricted Problem of Three Bodies*, Academic Press, New York, 1967.

[22]Broucke, R., "Stability of Periodic Orbits in the Elliptic, Restricted Three-Body Problem," *AIAA Journal*, Vol. 7, No. 6, 1969, pp. 1003–1009.

[23]Parker, T. S., and Chua, L. O., *Practical Numerical Algorithms for Chaotic Systems*, Springer-Verlag, New York, 1989, pp. 139–166.

[24]Chicone, C., *Ordinary Differential Equations with Applications*, Springer-Verlag, New York, 1999, pp. 162–176.

[25]Dunham, D. W., and Muhonen, D. P., "Tables of Libration-Point Parameters for Selected Solar System Objects," *Journal of the Astronautical Sciences*, Vol. 49, No. 1, 2002, pp. 197–217.

C. Kluever
Associate Editor